

Spiral wave chimera states in large populations of coupled chemical oscillators

Jan Frederik Tötz^{1*}, Julian Rode¹, Mark R. Tinsley², Kenneth Showalter^{2*} and Harald Engel^{1*}

The coexistence of coherent and incoherent dynamics in a population of identically coupled oscillators is known as a chimera state^{1,2}. Discovered in 2002³, this counterintuitive dynamical behaviour has inspired extensive theoretical and experimental activity^{4–15}. The spiral wave chimera is a particularly remarkable chimera state, in which an ordered spiral wave rotates around a core consisting of asynchronous oscillators. Spiral wave chimeras were theoretically predicted in 2004¹⁶ and numerically studied in a variety of systems^{17–23}. Here, we report their experimental verification using large populations of nonlocally coupled Belousov–Zhabotinsky chemical oscillators^{10,18} in a two-dimensional array. We characterize previously unreported spatiotemporal dynamics, including erratic motion of the asynchronous spiral core, growth and splitting of the cores, as well as the transition from the chimera state to disordered behaviour. Spiral wave chimeras are likely to occur in other systems with long-range interactions, such as cortical tissues²⁴, cilia carpets²⁵, SQUID metamaterials²⁶ and arrays of optomechanical oscillators⁹.

Experiments were carried out with a network of up to 1,600 photosensitive chemical oscillators, arranged in a 40 × 40 grid, photochemically coupled by specific illumination of each oscillator. The discrete micro-oscillators are catalyst-loaded ion-exchange beads, placed in catalyst-free Belousov–Zhabotinsky (BZ) solution^{10,18}. The experimental set-up (Fig. 1a) allowed the current state of each micro-oscillator to be monitored by using a camera to record its fluorescence intensity, which is linearly dependent on the concentration of the reduced form of the catalyst, Ru(dmbpy)₃²⁺ (see Methods and Supplementary Section ‘Experimental Setup’). The light intensity projected onto each oscillator was independently controlled using a spatial light modulator (SLM). The initial conditions for the experiment were set by individually forcing each oscillator with a periodic illumination intensity to align all of the oscillator phases to a desired phase distribution containing a phase singularity¹⁷. Once the desired phase alignment was attained, light-mediated nonlocal coupling was initiated between the oscillators in the network based on their state according to equation (1):

$$I_{j,k} = I_0 + K \sum_{m=j-l}^{j+l} \sum_{n=k-l}^{k+l} e^{-\kappa r} [g_{m,n}(t-\tau) - g_{j,k}(t)] \quad (1)$$

The light intensity projected on oscillator (j, k), at the centre of a square region of side length $2l+1$, is $I_{j,k}$. It is linearly dependent on the difference between the grey values $g_{j,k}$ and $g_{m,n}$ of oscillator (j, k) and the other oscillators (m, n) in the square region at times t and $(t-\tau)$, respectively (see Methods). This difference is weighted with a nonlocal coupling kernel that decays exponentially with

distance $r = \sqrt{(m-j)^2 + (n-k)^2}$ between oscillators (j, k) and (m, n). Parameters κ and K determine the coupling range and coupling strength³, respectively, and I_0 is the background illumination intensity. The time delay τ plays a role similar to the phase frustration parameter in the Kuramoto model²⁷.

A spiral wave chimera exhibiting the characteristic coexistence of coherent and incoherent oscillators is shown in Fig. 1, with an ordered spiral wave rotating around a core made up of asynchronous oscillators. Figure 1b shows a snapshot of the grey values and Fig. 1c shows the phase of each oscillator determined from the grey values. The periods of the incoherent oscillators in the core and the coherent oscillators in the spiral wave are plotted in Fig. 1d. For a time delay of $\tau = 2.0$ s, the rotation period T_{spiral} of the spiral arm is larger than the spatially averaged period T_{core} of the core oscillators. In contrast, at lower values of $\tau = 1.0$ s (Fig. 2b), the rotation period T_{spiral} is smaller than T_{core} . The space–time plot in Fig. 1e shows the spiral wave propagating out from the asynchronous core along the cross-section $j = 20$ in Fig. 1b during approximately five rotational periods of the spiral. The disordered core region exhibits a low degree of synchronization, as measured by the two-dimensional local Kuramoto order parameter $R_{j,k}$, defined as

$$R_{j,k} = \frac{1}{(2\delta+1)^2} \left| \sum_{m=j-\delta}^{j+\delta} \sum_{n=k-\delta}^{k+\delta} e^{i\varphi_{m,n}} \right| \quad (2)$$

where $\varphi_{m,n}$ represents the phases of oscillators (m, n) in a square region of side length $2\delta+1$ with oscillator (j, k) in the centre. We define a region of oscillators as asynchronous or incoherent in terms of the local order parameter, with $R_{j,k} < 0.4$; the value of $R_{j,k}$ in these regions, however, is typically lower. Over the course of the experiment, the core expands at ~ 300 s after its formation, doubling its size from ~ 20 to ~ 40 oscillators, and drifts until it collides with the upper boundary of the oscillator array and disappears at 1,040 s, or approximately 30 rotational periods (Supplementary Video 2).

Figure 2a–c shows the behaviour of a spiral wave chimera with a smaller value of time delay, $\tau = 1.0$ s. The erratic motion of the core can be characterized from the grey value data by calculating the trajectory of the core centre, defined as the location where the local order parameter $R_{j,k}$ reaches its weighted minimum value within the core (see Methods). A typical trajectory is shown in Fig. 2c. This erratic motion is in contrast to rigid or compound rotation known for spiral waves in reaction–diffusion systems²⁷.

With increasing delay time, $\tau = 5.0$ s, the core of the spiral wave chimera increases in size and eventually becomes unstable, leading to splitting of the core of asynchronous oscillators. An experimental example of core splitting in a spiral wave chimera is displayed in

¹Institut für Theoretische Physik, EW 7-1, TU Berlin, Hardenbergstr. 36, 10623 Berlin, Germany. ²C. Eugene Bennett Department of Chemistry, West Virginia University, Morgantown, WV 26506-6045, USA. *e-mail: jantotz@itp.tu-berlin.de; kenneth.showalter@mail.wvu.edu; h.engel@physik.tu-berlin.de

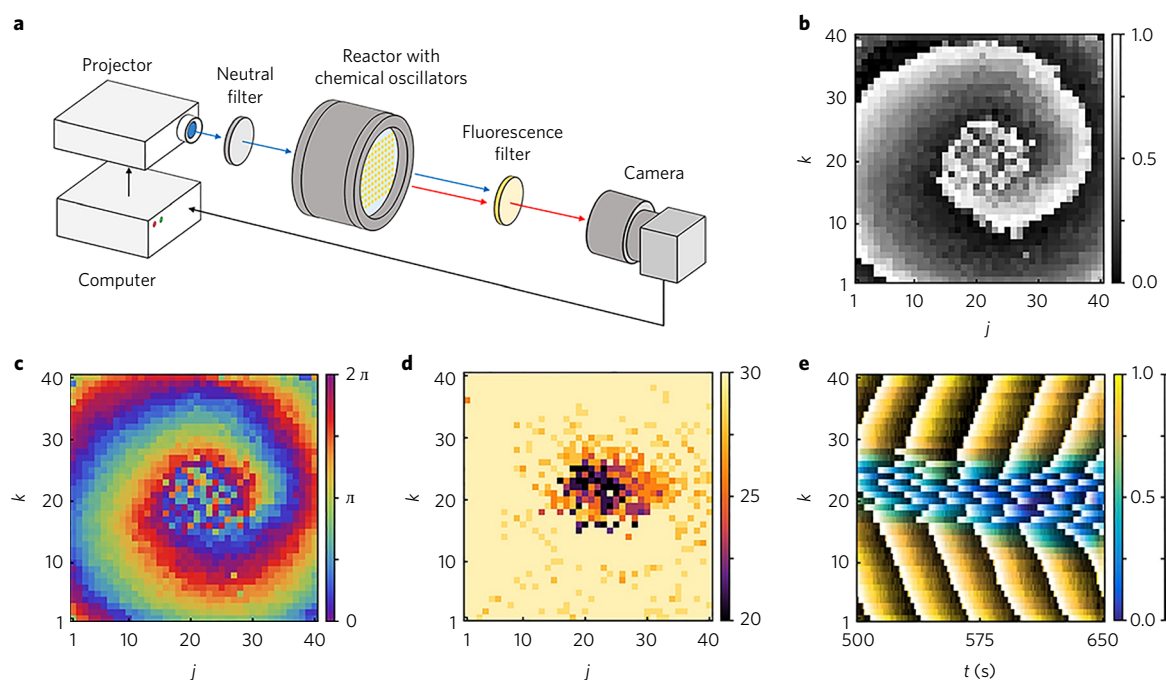


Fig. 1 | Experimental set-up and spiral wave chimera. **a**, The camera records fluorescent light ($\lambda > 500$ nm) emitted by the reduced form of the BZ catalyst ($\text{Ru}(\text{dmbpy})_3^{2+}$). The grey values corresponding to the concentration of the oxidized catalyst ($\text{Ru}(\text{dmbpy})_3^{3+}$) are used to determine the illumination intensity $I_{j,k}$ of oscillator (j, k) according to equation (1) (see Methods). The projector (Casio XJ-A140V) is fitted with 24 GaN laser diodes that illuminate at $\lambda = 440$ nm. **b**, Grey values of spiral wave chimera in an array of $N = 1,600$ photochemically coupled BZ oscillators (Supplementary Videos 1 and 2). The spiral rotates with period $T_{\text{spiral}} = 33$ s around the incoherent core consisting of approximately 40 phase-randomized oscillators. The image was taken 700 s after initiation of the spiral wave chimera. **c**, Oscillator phases obtained from the grey values in **b**. The instantaneous phases are calculated by linear interpolation between two consecutive peaks in the grey value time series. **d**, Period of the oscillators in **b**, illustrating that the spiral wave oscillators are approximately frequency-synchronized and phase-entrained in the rotating spiral wave, while the aperiodic core oscillators exhibit shorter periods. **e**, Space-time plot of the spiral wave chimera from measurements along the cross-section $j = 20$ in **b**, during five rotational periods of the spiral. The colour code indicates the value of the local order parameter calculated according to equation (2) with $\delta = 2$, and the level of brightness indicates the grey values as in **b**. The spiral core exhibits size fluctuations and undergoes erratic motion. Coupling parameters: $K = 0.08$, $\kappa = 3.1$, $\tau = 2.0$ s, $I_0 = 0.06$ mW cm $^{-2}$, $l = 4$. Initial reactant concentrations: $[\text{H}_2\text{SO}_4]_0 = 0.77$ M, $[\text{NaBrO}_3]_0 = 0.51$ M, $[\text{NaBr}]_0 = 0.08$ M, $[\text{malonic acid}]_0 = 0.16$ M. Average natural period and standard deviation: $T_0 = 85.7 \pm 8.3$ s.

Fig. 2d–f, where a single core sequentially splits to form the three cores depicted in the image. Figure 2d shows the phases of the oscillators, Fig. 2e gives the period of each oscillator and Fig. 2f shows the local order parameter, illustrating the low order associated with each spiral wave chimera core.

Further insights into the BZ spiral wave chimera can be gleaned from numerical simulations based on the ZBKE model²⁸ of the BZ reaction, modified to describe the discrete photosensitive BZ oscillator system¹⁰. Using the coupling scheme given by equation (1), the simulations generate spiral wave chimeras that are in excellent agreement with those found in the experiments (Supplementary Fig. 1). The simulations also provide information on the transition from relatively simple spiral wave chimera behaviour, such as that shown in Fig. 1, to more complex behaviour and ultimately to asynchronous behaviour as the value of time delay τ is increased.

Figure 3a shows the dependence of T_{spiral} and T_{core} on the delay time τ with all other model parameters held constant. Up to a delay time of $\tau \approx 6.3$, the value of T_{spiral} increases approximately linearly while T_{core} remains relatively constant. This is in agreement with the experimental behaviour, as previously mentioned, shown in Figs. 1d and 2b. Also shown in Fig. 3a is the fraction of the oscillator array that is made up of asynchronous oscillators as a function of τ . As τ increases we observe a sharp increase in the fraction of asynchronous oscillators for $\tau \geq 5.9$.

Figure 3b–i shows the time evolution of spiral wave chimeras for two values of τ in an array of nonlocally coupled BZ oscillators. The local order parameter $R_{j,k}$ at successive times is shown in Fig. 3b–e for $\tau = 6.2$. The core of the spiral wave chimera first increases in size and then splits into two cores. This process of core splitting continues until the domain is filled with spiral wave chimeras. The long-time behaviour is persistent but dynamic, as each spiral wave chimera core exhibits erratic movement and shape fluctuations. Spiral wave chimeras may also disappear on collision of the chimera core with a boundary (Supplementary Section ‘Boundary conditions’).

Figure 3f–i shows the very rapid growth of the core of a spiral wave chimera for larger delay time, $\tau = 6.6$, until asynchronous oscillators dominate the domain. Figure 3i shows the behaviour at $t = 1,740$, which can be compared with the behaviour at $t = 1,660$ in Fig. 3c for $\tau = 6.2$. At the higher value of τ , the expansion of the core is sufficiently rapid that core splitting events are apparently not possible. In other simulations, with the distribution of oscillator periods having the same standard deviation but being generated with a different random number seed, we found the same qualitative behaviour but with small quantitative shifts in the ranges of specific behaviours.

The process of a core of unsynchronized oscillators splitting into multiple cores involves the spontaneous formation of ordered, synchronized regions inside the core. These synchronized regions give

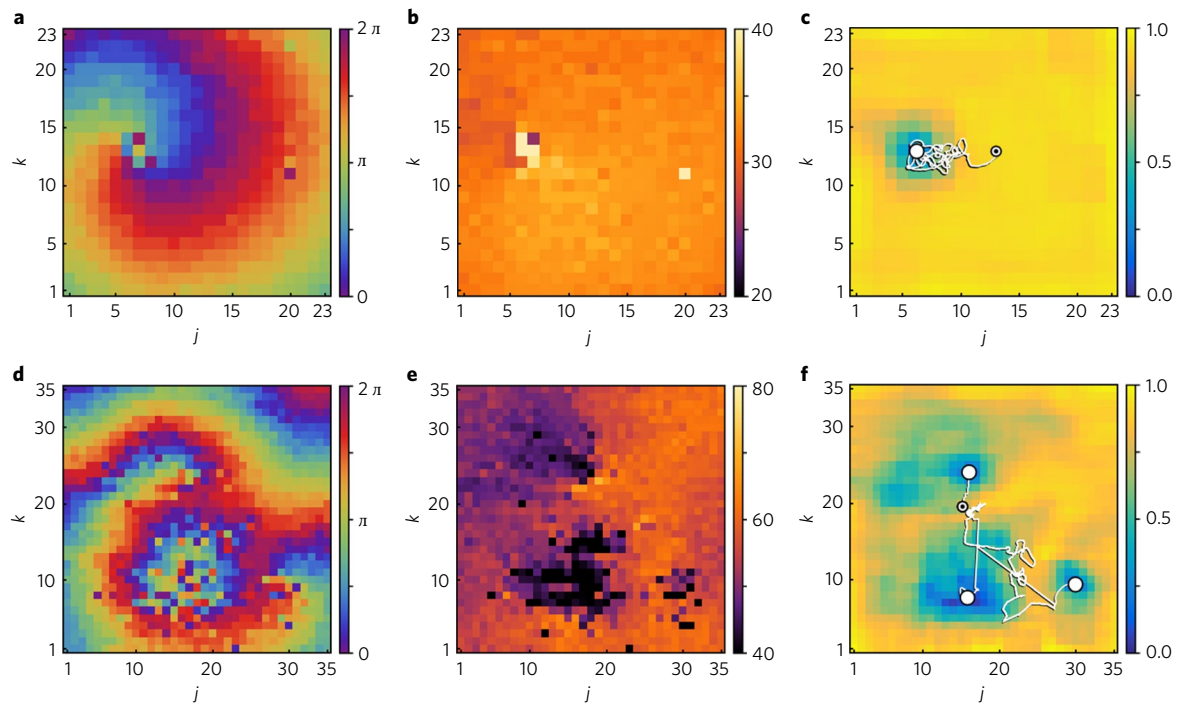


Fig. 2 | Core dynamics of spiral wave chimera. Experimental results for $\tau=1.0$ s (upper row) and $\tau=5.0$ s (bottom row). **a**, Oscillator phases of the spiral wave chimera (Supplementary Video 3). **b**, Period of oscillators in **a**, where the core oscillators have a mean period T_{core} of ~ 40 s, and the oscillators in the spiral arm exhibit a period T_{spiral} of ~ 30 s. **c**, Kuramoto local order parameter $R_{j,k}$ showing the core with low order for the spiral wave chimera depicted in **a**. Erratic movement of the core is indicated by the white line representing the trajectory of the location with minimum local order parameter $R_{j,k}$ (equation (2)). The initial core location is shown by the white circle with a central black dot. **d**, Oscillator phases showing growth and instability of a spiral wave chimera leading to core splitting (Supplementary Video 4). **e**, Period of oscillators in **d**, where the period in each core is shorter than the period of the oscillators surrounding the core. **f**, Kuramoto local order parameter $R_{j,k}$ showing the separated cores with low order for the spiral wave chimeras depicted in **d**, as well as the trajectories of each core after a splitting event. Experimental parameters are as in Fig. 1. Average natural period and standard deviation: $T_0=54.8 \pm 1.4$ s (**a-c**) and $T_0=84.8 \pm 8.1$ s (**d-f**).

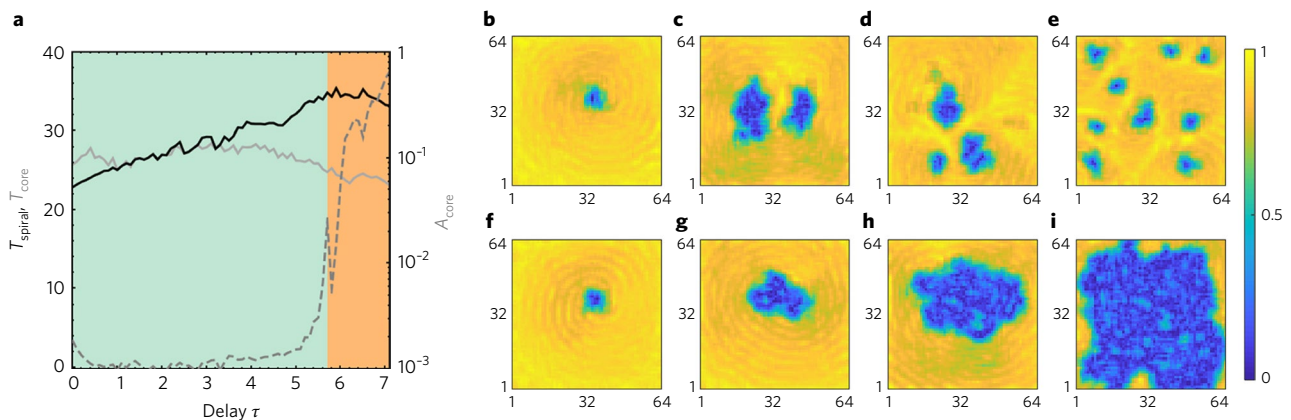


Fig. 3 | Splitting of spiral wave chimera cores and transition to incoherence. **a**, Simulations showing the dependence on the delay time τ of the time-averaged period of the spiral wave oscillators, T_{spiral} (solid black line), the relatively constant time-averaged period of the incoherent core oscillators, T_{core} (solid grey line), and the time-averaged fraction of the network made up of incoherent oscillators, A_{core} (dashed grey line). The value of A_{core} is given by the relative number of oscillators with the local order parameter $R_{j,k} < 0.4$. The sharp increase in the fraction of the oscillators exhibiting asynchronous behaviour can be seen in the salmon-coloured region of the plot. The simulations were carried out with a 64×64 oscillator array using the ZBKE model modified to describe the photosensitive BZ oscillator system (see Supplementary Section ‘Numerical Models’). **b-e**, Numerical simulations of splitting and growth of the spiral wave chimera (Supplementary Video 5). An initially small spiral wave chimera in the centre of the network undergoes growth and then splitting. Each new core is capable of further growth and splitting. In **e**, the long-term behaviour is dynamical in nature, with small spiral wave chimeras filling the domain, but with each in continuous motion and exhibiting shape fluctuations. The local order parameter $R_{j,k}$ is shown in **b-e** at times 250, 1,660, 2,219 and 8,500. **f-i**, An initially small spiral wave chimera grows rapidly without splitting until it eventually occupies the majority of the network (Supplementary Video 6). The local order parameter $R_{j,k}$ is shown in **f-i** for times 250, 520, 750 and 1,740, respectively. The time delay for **b-e** is $\tau=6.2$ and for **f-i** is $\tau=6.6$. Average natural period and standard deviation: $T_0=36.0 \pm 1.6$ (All times t , delay times τ and periods T_0 are dimensionless from the non-dimensionalized ZBKE model.).

rise to core splitting into separate cores as well as to the initiation of new wave segments. Careful examination of the time evolution of the spiral wave chimera core splitting reveals that topological charge²⁹ is preserved in the process (Supplementary Section ‘Spiral wave chimera core splitting’).

The phase response curves (PRCs) for both the experimental and model systems provide insights into the transient order in the core (Supplementary Fig. 4). The PRC displays the features of the relaxation oscillations exhibited by the BZ reaction. Oscillators with phases that are in the region ranging from approximately π to 2π fire immediately when sufficiently perturbed, creating transient localized phase alignment.

Our studies suggest that the spiral wave chimeras, core expansion and core splitting observed in the BZ system are likely to be found in a range of other systems with the common properties of immediate firing following a perturbation and long-range interactions. For example, we have found similar spiral wave chimera behaviour, with core splitting and the transition to predominantly asynchronous behaviour, in populations of nonlocally coupled FitzHugh–Nagumo oscillators (Supplementary Fig. 3). The PRC for the FitzHugh–Nagumo system resembles the PRC of the BZ system and ZBKE model, with an immediate firing region (Supplementary Fig. 4). Pulse coupled oscillator models of neuronal systems can also have immediate firing dynamics³⁰, suggesting that certain neuronal networks might exhibit spiral wave chimera behaviour similar to that described here. Other possible systems where these behaviours might be found include biological tissues^{24,25} and arrays of physical oscillators^{9,26}.

Received: 12 June 2017; Accepted: 6 October 2017;
Published online: 4 December 2017

References

- Abrams, D. M. & Strogatz, S. H. Chimera states for coupled oscillators. *Phys. Rev. Lett.* **93**, 174102 (2004).
- Panaggio, M. J. & Abrams, D. M. Chimera states: coexistence of coherence and incoherence in networks of coupled oscillators. *Nonlinearity* **28**, R67 (2015).
- Kuramoto, Y. & Battogtokh, D. Coexistence of coherence and incoherence in nonlocally coupled phase oscillators. *Nonlin. Phenom. Complex Syst.* **5**, 380–385 (2002).
- Zakharova, A., Kapeller, M. & Schöll, E. Chimera death: symmetry breaking in dynamical networks. *Phys. Rev. Lett.* **112**, 154101 (2014).
- Abrams, D. M., Mirollo, R., Strogatz, S. H. & Wiley, D. A. Solvable model for chimera states of coupled oscillators. *Phys. Rev. Lett.* **101**, 084103 (2008).
- Wolfgram, M. & Omel'chenko, O. E. Chimera states are chaotic transients. *Phys. Rev. E* **84**, 015201 (2011).
- Sethia, G. C., Sen, A. & Atay, F. M. Clustered chimera states in delay-coupled oscillator systems. *Phys. Rev. Lett.* **100**, 144102 (2008).
- Schmidt, L., Schönleber, K., Krischer, K. & García-Morales, V. Coexistence of synchrony and incoherence in oscillatory media under nonlinear global coupling. *Chaos* **24**, 013102 (2014).
- Hagerstrom, A. M. et al. Experimental observation of chimeras in coupled-map lattices. *Nat. Phys.* **8**, 658–661 (2012).
- Tinsley, M. R., Nkomo, S. & Showalter, K. Chimera and phase-cluster states in populations of coupled chemical oscillators. *Nat. Phys.* **8**, 662–665 (2012).
- Martens, E. A., Thutupalli, S., Fourrière, A. & Hallatschek, O. Chimera states in mechanical oscillator networks. *Proc. Natl Acad. Sci. USA* **110**, 10563–10567 (2013).
- Wojewoda, J., Czolczynski, K., Maistrenko, Y. & Kapitaniak, T. The smallest chimera state for coupled pendula. *Sci. Rep.* **6**, 34329 (2016).
- Wickramasinghe, M. & Kiss, I. Z. Spatially organized dynamical states in chemical oscillator networks: synchronization, dynamical differentiation, and chimera patterns. *PLoS ONE* **8**, e80586 (2013).
- Larger, L., Penkovsky, B. & Maistrenko, Y. Laser chimeras as a paradigm for multistable patterns in complex systems. *Nat. Commun.* **6**, 7752 (2015).
- Rosin, D. P., Rontani, D., Haynes, N. D., Schöll, E. & Gauthier, D. J. Transient scaling and resurgence of chimera states in networks of Boolean phase oscillators. *Phys. Rev. E* **90**, 030902 (2014).
- Shima, S. & Kuramoto, Y. Rotating spiral waves with phase-randomized core in nonlocally coupled oscillators. *Phys. Rev. E* **69**, 036213 (2004).
- Martens, E. A., Laing, C. R. & Strogatz, S. H. Solvable model of spiral wave chimeras. *Phys. Rev. Lett.* **104**, 044101 (2010).
- Nkomo, S., Tinsley, M. R. & Showalter, K. Chimera states in populations of nonlocally coupled chemical oscillators. *Phys. Rev. Lett.* **110**, 244102 (2013).
- Gu, C., St-Yves, G. & Davidsen, J. Spiral wave chimeras in complex oscillatory and chaotic systems. *Phys. Rev. Lett.* **111**, 134101 (2013).
- Tang, X. et al. Novel type of chimera spiral waves arising from decoupling of a diffusible component. *J. Chem. Phys.* **141**, 024110 (2014).
- Xie, J. B., Knobloch, E. & Kao, H. C. Twisted chimera states and multicore spiral chimera states on a two-dimensional torus. *Phys. Rev. E* **92**, 042921 (2015).
- Lau, H. W. & Davidsen, J. Linked and knotted chimera filaments in oscillatory systems. *Phys. Rev. E* **94**, 010204 (2016).
- Laing, C. R. Chimeras in two-dimensional domains: heterogeneity and the continuum limit. *SIAM J. Appl. Dyn. Sys.* **16**, 974–1014 (2017).
- Huang, X. et al. Spiral waves in disinhibited mammalian neocortex. *J. Neurosci.* **24**, 9897–9902 (2004).
- Uchida, N. & Golestanian, R. Synchronization and collective dynamics in a carpet of microfluidic rotors. *Phys. Rev. Lett.* **104**, 178103 (2010).
- Lazarides, N., Neofotistos, G. & Tsironis, G. P. Chimeras in SQUID metamaterials. *Phys. Rev. B* **91**, 054303 (2015).
- Winfree, A. T. *The Geometry of Biological Time* (Springer, New York, 2001).
- Zhabotinsky, A. M., Buchholtz, F., Kiyatkin, A. B. & Epstein, I. R. Oscillations and waves in metal-ion-catalyzed bromate oscillating reactions in highly oxidized states. *J. Phys. Chem.* **97**, 7578–7584 (1993).
- Davidsen, J., Glass, L. & Kapral, R. Topological constraints on spiral wave dynamics in spherical geometries with inhomogeneous excitability. *Phys. Rev. E* **70**, 056203 (2004).
- Canavier, C. C. & Achuthan, S. Pulse coupled oscillators and the phase resetting curve. *Math. Biosci.* **226**, 77–96 (2010).

Acknowledgements

The authors thank J. Sixt and F. Sielaff from TU Berlin Physics Department's precision mechanical workshop for preparing the acrylic glass plates with micrometre-sized cavities that hold the micro-oscillators and U. Künkel for assistance in the laboratory. This work was supported by the Deutsche Forschungsgemeinschaft (grants GRK 1558 and SFB 910 to J.F.T., J.R. and H.E.), the National Science Foundation (grant CHE-1565665 to K.S. and M.R.T.) and the Alexander von Humboldt-Stiftung (to K.S.).

Author contributions

J.F.T. and J.R. built and programmed the set-up and performed experiments. J.F.T., K.S. and H.E. designed the study and wrote the paper. The simulations were carried out by J.F.T. and J.R., except for those shown in Fig. 3b–i, which were done by M.R.T. All authors discussed the results and commented on the manuscript.

Competing interests

The authors declare no competing financial interests.

Additional information

Supplementary information is available for this paper at <https://doi.org/10.1038/s41567-017-0005-8>.

Reprints and permissions information is available at www.nature.com/reprints.

Correspondence and requests for materials should be addressed to J.F.T. or K.S. or H.E.

Publisher's note: Springer Nature remains neutral with regard to jurisdictional claims in published maps and institutional affiliations.

Methods

Experiments. The chemical micro-oscillators used in this study are catalyst-loaded cation-exchange beads in a catalyst-free BZ reaction mixture^{10,18,31–33}. To increase oscillator homogeneity, the particles (DOWEX WX4 100–200, diameters 75–150 μm) were sieved to obtain a narrow size distribution of 106–112 μm . The ruthenium-tris-dimethylene-bipyridine ($\text{Ru}(\text{dmbpy})_3^{2+}$) catalyst was slowly added to 5.0 ml water containing 1.0 g of doubly-sieved beads and stirred with a vortex mixer for one day. For storage purposes the beads were filtered and dried. The dimethylene ligands of the ruthenium complex lead to greater stability of the catalyst in the bead-polymer matrix. The beads were wetted with a water-methanol solution and distributed onto wells of depth 150 μm drilled into an acrylic plate. Once the solution had evaporated, silica hydrogel and surfactant (Triton X-100) were applied to the surface in a spray. The acrylic glass, with an array of 2,816 chemical oscillators, was mounted in a thermostatted reactor, and 1,600 oscillators were selected that fell in a narrow period distribution. The oscillators were sufficiently separated (400 μm) to exclude diffusive coupling. Each oscillator was individually illuminated with a light intensity based on the oxidation state of oscillators in its neighbourhood, according to equation (1). The coupling was updated every 1.0 s.

Grey value. The fluorescence of the reduced catalyst ($\text{Ru}(\text{dmbpy})_3^{2+}$) was monitored in the experiments, giving its concentration. However, the sharp rise in the leading edge of the spiral wave occurs with an increase of the oxidized catalyst ($\text{Ru}(\text{dmbpy})_3^{3+}$) corresponding to the oscillators firing. Because the sum of the concentrations of the two forms of the catalyst is a constant, $[\text{Ru}(\text{II})] + [\text{Ru}(\text{III})] = \text{total catalyst}$, we can obtain the grey values corresponding to the concentration of Ru(III) by calculating the normalized complement of the measured grey values: $g_{\text{ox}} = 1 - g_{\text{red}}$, where g_{ox} and g_{red} are the grey values corresponding to the concentrations of the oxidized catalyst [Ru(III)] and reduced catalyst [Ru(II)]. We use the grey values g_{ox} for $g_{j,k}$ and $g_{m,n}$ in equation (1).

Core tracking. The core centre position used for tracking was obtained by evaluating the weighted minimum in the local order parameter field. Core splitting

events require the algorithm to track new spiral cores. This was achieved by tracking connected sets of cells for which the local order parameter $R_{j,k}$ was less than 0.4 and calculating their centroids.

Initial conditions. The initial conditions in the experiments and simulations are given by the phase distribution $\varphi_{j,k} = \arctan[(k - k_0)/(j - j_0)]$, with (j_0, k_0) being the centre of the spiral.

Simulations. We used the non-dimensionalized ZBKE model^{10,28,31} (see Supplementary Section 'Numerical models') with a rectangular distribution in the parameter $q \in [0.6, 0.8]$ that leads to a heterogeneous period distribution with a standard deviation of 4.4% of the mean period. Nonlocal coupling was applied to each oscillator via the model parameter $I_{j,k}$ in a similar manner to equation (1), but with the measured greyscale value $g_{j,k}$ replaced by the oxidized catalyst concentration of the model. The resulting equations were integrated in time with a forward Euler solver in CUDA on a graphics card (Nvidia GTX 970).

Code availability. The numerical simulation code is available on a public Git repository: https://github.com/bzjan/Spiral_Wave_Chimera_Solver.git

Data availability. The data that support the plots within this paper and other findings of this study are available from the corresponding authors upon request.

References

- Taylor, A. F. et al. Clusters and switchers in globally coupled photochemical oscillators. *Phys. Rev. Lett.* **100**, 214101 (2008).
- Totz, J. F. et al. Phase-lag synchronization in networks of coupled chemical oscillators. *Phys. Rev. E* **92**, 022819 (2015).
- Nkomo, S., Tinsley, M. R. & Showalter, K. Chimera and chimera-like states in populations of nonlocally coupled homogeneous and heterogeneous chemical oscillators. *Chaos* **26**, 094826 (2016).